

Cite this: *Nanoscale*, 2012, **4**, 7021

www.rsc.org/nanoscale

PAPER

## Anticancer effect and mechanism of polymer micelle-encapsulated quercetin on ovarian cancer

Xiang Gao,<sup>ab</sup> BiLan Wang,<sup>a</sup> XiaWei Wei,<sup>a</sup> Ke Men,<sup>a</sup> Fengjin Zheng,<sup>b</sup> Yingfeng Zhou,<sup>c</sup> Yu Zheng,<sup>a</sup> MaLing Gou,<sup>\*a</sup> Meijuan Huang,<sup>a</sup> Gang Guo,<sup>a</sup> Ning Huang,<sup>b</sup> ZhiYong Qian<sup>a</sup> and Yuquan Wei<sup>a</sup>

Received 7th August 2012, Accepted 7th September 2012

DOI: 10.1039/c2nr32181e

Encapsulation of hydrophobic agents in polymer micelles can improve the water solubility of cargos, contributing to develop novel drugs. Quercetin (QU) is a hydrophobic agent with potential anticancer activity. In this work, we encapsulated QU into biodegradable monomethoxy poly(ethylene glycol)-poly( $\epsilon$ -caprolactone) (MPEG-PCL) micelles and tried to provide proof-of-principle for treating ovarian cancer with this nano-formulation of quercetin. These QU loaded MPEG-PCL (QU/MPEG-PCL) micelles with drug loading of 6.9% had a mean particle size of 36 nm, rendering the complete dispersion of quercetin in water. QU inhibited the growth of A2780S ovarian cancer cells on a dose dependent manner *in vitro*. Intravenous administration of QU/MPEG-PCL micelles significantly suppressed the growth of established xenograft A2780S ovarian tumors through causing cancer cell apoptosis and inhibiting angiogenesis *in vivo*. Furthermore, the anticancer activity of quercetin on ovarian cancer cells was studied *in vitro*. Quercetin treatment induced the apoptosis of A2780S cells associated with activating caspase-3 and caspase-9. MCL-1 downregulation, Bcl-2 downregulation, Bax upregulation and mitochondrial transmembrane potential change were observed, suggesting that quercetin may induce apoptosis of A2780S cells through the mitochondrial apoptotic pathway. Otherwise, quercetin treatment decreased phosphorylated p44/42 mitogen-activated protein kinase and phosphorylated Akt, contributing to inhibition of A2780S cell proliferation. Our data suggested that QU/MPEG-PCL micelles were a novel nano-formulation of quercetin with a potential clinical application in ovarian cancer therapy.

### 1. Introduction

The American Cancer Society estimated that ovarian cancer accounted for approximately 3% of all cancer diagnoses among American women.<sup>1</sup> Worldwide, ovarian cancer accounted for 4% of female cancer cases and is the main cause of death among gynecological cancers.<sup>2</sup> It is estimated that there will be approximately 22 280 new cases of ovarian cancer and 15 500 deaths from ovarian cancer in the United States in 2012.<sup>3</sup> Consistent evidence indicates that increasing age, family history of ovarian cancer, nulliparity, early menarche and late menopause were known risk factors for ovarian cancer, while the use of oral contraceptives, pregnancy, breastfeeding and tubal ligation decreases ovarian cancer risk.<sup>4</sup>

The efficacy of various currently available therapeutic strategies for ovarian cancer is not always sufficient, especially for advanced disease because symptoms of ovarian cancer were thought not to present until late stages.<sup>5</sup> Despite the evolution of surgical techniques and meticulously designed chemotherapy regimens, relapse remains almost inevitable in patients with advanced disease. Though there are many chemical therapeutic drugs for treatment of ovarian cancer, they usually exhibit various side effects.<sup>6–8</sup> Therefore, it is interesting to find natural drugs with little toxicity, and make great progress for ovarian cancer therapy using system administration.

Quercetin is a polyphenolic compound widely distributed in many plants, such as apple and tea. Its molecular structure is

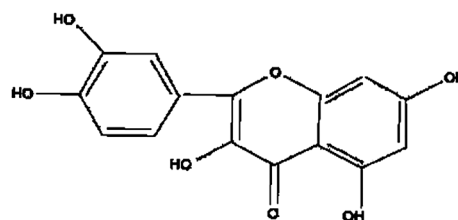


Fig. 1 The molecular structure of quercetin.

<sup>a</sup>State Key Laboratory of Biotherapy and Cancer Center, West China Hospital, West China Medical School, Sichuan University, Chengdu 610041, People's Republic of China. E-mail: basad@163.com

<sup>b</sup>Medical School and Department of Pathophysiology, College of Preclinical and Forensic Medical Sciences, Sichuan University, Chengdu 610041, People's Republic of China

<sup>c</sup>First Affiliated Hospital, Xixiang Medical School, Xixiang, 453003, People's Republic of China

presented in Fig. 1. Recent studies indicated that quercetin has promising applications in cancer therapy,<sup>9–11</sup> as well as anti-inflammatory properties.<sup>12</sup> It was reported that quercetin could inhibit the growth of cancer cells through inducing apoptosis in a variety of cancer cell lines.<sup>13</sup> Many tumor cells were arrested in a cycle by quercetin, such as G2/M arrest in lung and laryngeal or G1 arrest in colon and gastric cancer cells, as well as in leukaemic cells.<sup>14–18</sup> Moreover, quercetin-induced apoptosis may result from the induction of stress proteins, disruption of microtubules and mitochondria, release of cytochrome c, and activation of caspases.<sup>9,19–21</sup> However, the effects of quercetin on ovarian cancer are rarely investigated. Therefore, it is interesting to study the anticancer effect and mechanism of quercetin on ovarian cancer.

Despite the promising application of quercetin in cancer therapy, but the clinical use of quercetin was restricted because of the poor water solubility. Thus a novel aqueous formulation of quercetin was desirable. Nanotechnology provides a novel platform to overcome the poor water solubility of lipophilic drugs.<sup>22–24</sup> Encapsulation of hydrophobic drugs into nanoparticles can make the drug completely dispersible in water, making the drug intravenously injectable. Biodegradable polymeric nanoparticles are viewed as excellent candidates for anticancer drug delivery systems.<sup>25,26</sup> Some biodegradable polymer nanoparticle-delivered anticancer drugs are already in clinical study or marketed. Poly( $\epsilon$ -caprolactone)/poly(ethylene glycol) (PCL/PEG) block copolymers are biodegradable, amphiphilic and easy to produce, showing promising applications in drug delivery systems.<sup>27,28</sup> In recent years using PCL/PEG nanoparticles to encapsulate drugs to improve the water solubility of hydrophobic drug has attracted some attention.

In this work, the effect of quercetin on the proliferation and colony formation ability of human ovarian cells was examined in detail. Furthermore, we examined the effect and mechanism of quercetin on the incidence of apoptosis. In order to better evaluate the anti-tumor efficacy of quercetin *in vivo*, we encapsulate quercetin in MPEG-PCL micelles to meet the requirement of intravenous administration. Also, the anticancer effect of QU/MPEG-PCL micelles was evaluated *in vivo*. These results suggested that QU/MPEG-PCL micelles are an interesting nanoformulation of quercetin with potential application in ovarian cancer therapy.

## 2. Materials and methods

### 2.1 Materials

Hoechst 33342, quercetin, and 3-(4,5-dimethylthiazol-2-yl)2,5-diphenyltetrazolium bromide (MTT) were purchased from Sigma. Anti-MCL-1, anti-caspase-3, anti-caspase-9, anti-bcl-2, anti-bax, anti-MAPK, anti-p-MAPK, anti-Akt, anti-p-Akt, anti-GAPDH and horseradish peroxidase-conjugated goat anti-rabbit IgG antibodies were purchased from Cell Signaling Technology (CST). Dulbecco's modified Eagle medium (DMEM) medium was from Gibco BRL (Invitrogen Co, Carlsbad, CA). Fetal bovine serum was from Hangzhou Sijiqing Biotechnology (Hangzhou, China).

Seven-week-old female BALB/c athymic nude mice (Beijing animal center, Beijing, China) were used in the present study. All animal procedures were performed following the protocol

approved by the Institutional Animal Care and Treatment Committee of Sichuan University (Chengdu, P.R. China). All mice were treated humanely throughout the experimental period.

### 2.2 Preparation and characterization of QU/MPEG-PCL micelles

QU/MPEG-PCL micelles were prepared by a self-assembly method.<sup>29</sup> Briefly, quercetin (7 mg) and MPEG-PCL diblock copolymer (93 mg) were co-dissolved in the organic solution (4 mL of dichloromethane and 2 mL of methanol), followed by evaporation of this solution under reduced pressure in a rotary evaporator at 55 °C. Then, normal saline was added into the mixture, allowing the self-assembly of MPEG-PCL and QU, creating core-shell structured QU/MPEG-PCL micelles with core-encapsulated quercetin.

The preparation of empty MPEG-PCL micelles was the by the same method as the QU/MPEG-PCL micelles without quercetin in the mixtures.

The particle size and zeta potential of QU/MPEG-PCL micelles was determined by dynamic light scattering (Malvern Nano-ZS 90). The temperature was kept at 25 °C during the measuring process. All results were the mean of 3 test runs.

The morphology of QU/MPEG-PCL micelles was observed under a transmission electron microscope (TEM) (H-6009IV, Hitachi, Japan): micelles were diluted with distilled water and placed on a copper grid covered with nitrocellulose. Samples were negatively stained with phosphotungstic acid and dried at room temperature.

Drug loading (DL) and encapsulation efficiency (EE) of QU/MPEG-PCL micelles were determined as follows. Briefly, 10 mg of lyophilized QU/MPEG-PCL micelles were dissolved in 0.1 mL dichloromethane (DCM) and diluted with methanol. The amount of quercetin in the solution was determined by HPLC.<sup>29</sup> The DL and EE of QU/MPEG-PCL micelles were calculated according to eqn (1) and (2):

$$DL = \frac{\text{Drug}}{\text{polymer} + \text{Drug}} \times 100\% \quad (1)$$

$$EE = \frac{EDL}{TDL} \times 100\% \quad (2)$$

DL: drug loading, EE: encapsulation efficiency, EDL: experimental drug loading, TDL: theoretical drug loading.

### 2.3 Cell culture

Human ovarian cancer cells A2780S cells were obtained from American Type Culture Collection and cultured in DMEM medium supplemented with 10% FBS (CC medium), 1% penicillin and streptomycin (growth medium) at 37 °C in a 5% CO<sub>2</sub> incubator.

### 2.4 Cell viability and proliferation

To study the effects of quercetin on cell proliferation and viability, A2780S cell lines ( $5 \times 10^3$  per well) were plated in 96-well plates and incubated in CC medium. After 24 h, cells were washed once with medium and treated with 0, 0.12, 0.23, 0.47, 0.94, 1.88, 3.725, 7.5, 15 and 30  $\mu\text{g mL}^{-1}$  quercetin in medium.

Cell proliferation and cell viability were determined after 24 h or 48 h of treatment by incubation in CC medium containing 0.5 mg mL<sup>-1</sup> MTT for 4 h. The surviving cells converted MTT to formazan, which generates a blue-purple color when dissolved in dimethyl sulfoxide (DMSO). The color intensity was measured at 570 nm using a plate reader (OPTImax, Molecular Dynamics). Experiments were repeated at least three times, and the data were expressed as mean  $\pm$  SD.

## 2.5 Colony formation assay

Approximately 400 A2780S cells were cultured in six-well plate at 37 °C and 5% CO<sub>2</sub> in a humidified incubator. Twenty four hours later, cells were treated with different concentrations of quercetin (0, 7.5, 15 and 30  $\mu$ g mL<sup>-1</sup>) for another 24 h. Then, cells were washed twice with PBS and re-cultured in CC medium for 14 days. The cells were harvested for colony formation. Colonies were fixed with methanol, treated with Giemsa stain, and counted by using image analysis software. Photographs were taken using a digital camera (Canon, Tokyo, Japan).

## 2.6 Evaluation of the anticancer effect of QU/MPEG-PCL micelles *in vivo*

A2780S cells ( $1 \times 10^7$ ) were inoculated in the subcutaneous tissue of mice. When tumors grew to approximately 100 mm<sup>3</sup>, mice were randomly divided into two groups (5 mice per group). QU/MPEG-PCL (QU: 60 mg kg<sup>-1</sup>) or empty MPEG-PCL (Control) were intravenously administered. Tumor volumes were assessed by bilateral Vernier calliper measurement every three days and calculated according to the equation: [tumor volume =  $a^2 \times b \times 0.52$ ], where  $a$  represented the shorter and  $b$  represented the longer of the two dimensions. Body weight was measured every three days and clinical symptoms were observed daily.

## 2.7 Histology and apoptosis analysis

A commercially available TUNEL kit (Promega, Madison, WI) was used to analyze apoptotic cells within A2780S tumors. This analysis was performed following the manufacturer's protocol; these samples were examined with a fluorescence microscope ( $\times 400$ ).

For blood vessel staining, tumors were stored at  $-80$  °C to examine the microvessel expression, immunostained with epithelial cell marker goat anti-mouse CD31 antibody (dilution 1 : 50; Santa Cruz Biotechnology) overnight at 4 °C, then rabbit-anti-goat FITC (dilution 1 : 100; Santa Cruz Biotechnology) was added and the samples left in a humidified chamber protected from light at 37 °C for 1 h. The microvessel density was determined as the average number of CD31-positive small vessels in a high-power ( $\times 400$ ) field.

## 2.8 Cell apoptosis analysis

**2.8.1 Morphological analysis after Hoechst staining.** To investigate the apoptosis induction effect of quercetin, we analyzed the apoptotic cells by Hoechst staining. Briefly, A2780S cells were seeded in 6-well plates for 24 h. After quercetin treatment for another 48 h, cells were stained with Hoechst 33342 solutions (5  $\mu$ g mL<sup>-1</sup>) in 0.1% sodium citrate. Then nuclear

morphology of cells was examined with inverted fluorescence microscopy (Zeiss, Axiovert 200, Germany).

**2.8.2 Apoptosis analysis by flow cytometry (FCM).** The extent of apoptosis in A2780S was evaluated by flow cytometric (FCM: BD FACSCalibur, USA) analysis using FITC-conjugated AnnexinV/propidium iodide (PI; BD PharMingen) staining according to the manufacturer's instructions.<sup>30</sup> Both early apoptotic (Annexin V-positive, PI-negative) and late apoptotic (Annexin V-positive and PI-positive) cells were included in cell death determinations.

## 2.9 Mitochondrial membrane potential change assay

Quercetin-induced change of the mitochondrial membrane potential was evaluated by FCM using rhodamine 123 (Rh123), as described previously.<sup>31</sup> Cell culture and drug treatment were done as described above. A2780s were incubated with 5  $\mu$ g mL<sup>-1</sup> of Rh123 for 30 min in the dark. Then fluorescence emitted from the Rh123 was detected by FCM.

## 2.10 Western blotting

Western blotting analysis was performed using standard methods.<sup>32</sup> Cell culture and drug treatment were done as described above. Cell lysates were washed twice with PBS and lysed in RIPA (radioimmunoprecipitation assay) buffer. Then lysates were centrifuged at 12 000g for 30 min at 4 °C. The supernatants were centrifuged at 10 000g for 15 min at 4 °C. Then, the mitochondrial pellets and aliquots of the supernatant (cytosolic fraction) were collected. The samples were quantitative with Bio-Rad Protein Assay kit (Bio-Rad Laboratories), dissolved in 6 $\times$  SDS sample buffer and denatured, then subjected to SDS-PAGE (sodium dodecyl sulfate polyacrylamide gel electrophoresis) and transferred onto PVDF (polyvinylidene fluoride) (Bio-Rad, Hercules, CA) membranes, then incubated overnight at 4 °C with the respective primary antibodies and horseradish peroxidase-conjugated secondary antibodies. Protein bands were visualized using a commercially available enhanced chemiluminescence kit (Amersham Biosciences Corp., Piscataway, NJ).

## 2.11 Statistical analysis

Data were expressed as the mean value  $\pm$  sd. Statistical analysis was performed with one-way analysis of variance (ANOVA) using SPSS software.  $P$  values less than 0.05 was considered to be statistically significant.

## 3. Results

In this manuscript, the anticancer activity and mechanism of quercetin on A2780S ovarian cancer cells was studied *in vitro*. Furthermore, a novel nano-formulation of quercetin (QU/MPEG-PCL micelles) was prepared and used to treat ovarian cancer *in vivo*. This work may provide a proof-of-principle for treating ovarian cancer with QU/MPEG-PCL micelles.

### 3.1. Preparation and characterization of the QU/MPEG-PCL micelles

In order to improve the water solubility of quercetin, MPEG-PCL was employed to encapsulate quercetin. QU/MPEG-PCL micelles were prepared by self-assembly, as previously reported.<sup>29</sup> Briefly, 7 mg quercetin and 93 mg MPEG-PCL were co-dissolved into the mixture of DCM and methanol. Then the organic mixture was evaporated under pressure, forming an MPEG-PCL and QU mixture. Finally, normal saline solution was added to the mixture, allowing the self-assembly of MPEG-PCL and QU in solution. In the structure of MPEG-PCL, PEG is the hydrophilic segment and PCL is the hydrophobic segment; thus, MPEG-PCL micelles always have a core-shell structure in water, with a PCL core and a PEG shell. The self-assembly of MPEG-PCL and QU created core-shell QU/MPEG-PCL micelles with core-encapsulated QU (Fig. 2A).

The QU/MPEG-PCL micelles were characterized in detail. The QU/MPEG-PCL micelles had DL and EE of 6.9% and 98.1%, respectively. The zeta potential spectrum of QU/MPEG-PCL micelles is presented in Fig. 2B; QU/MPEG-PCL micelles had a zeta potential of  $-2.69 \pm 0.45$  mV. In Fig. 2C, the particle size distribution spectrum of freshly prepared QU/MPEG-PCL micelles are presented. It was indicated that QU/MPEG-PCL micelles had a very narrow particle size distribution (polydispersity index [PDI] =  $0.13 \pm 0.04$ ) with a mean particle size of  $36.1 \pm 3.2$  nm (determined by DLS). Moreover, the morphology of QU/MPEG-PCL micelles was studied by transmission electron microscopy (TEM), and the result is shown in Fig. 2D. According to the TEM image, QU/MPEG-PCL micelles were spherical with a mean diameter of  $\sim 23$  nm. TEM determined the size of dry particles, while the DLS determined the hydrodynamic diameter of particles in water. Because amphiphilic block polymeric micelles always have a loose structure in water,

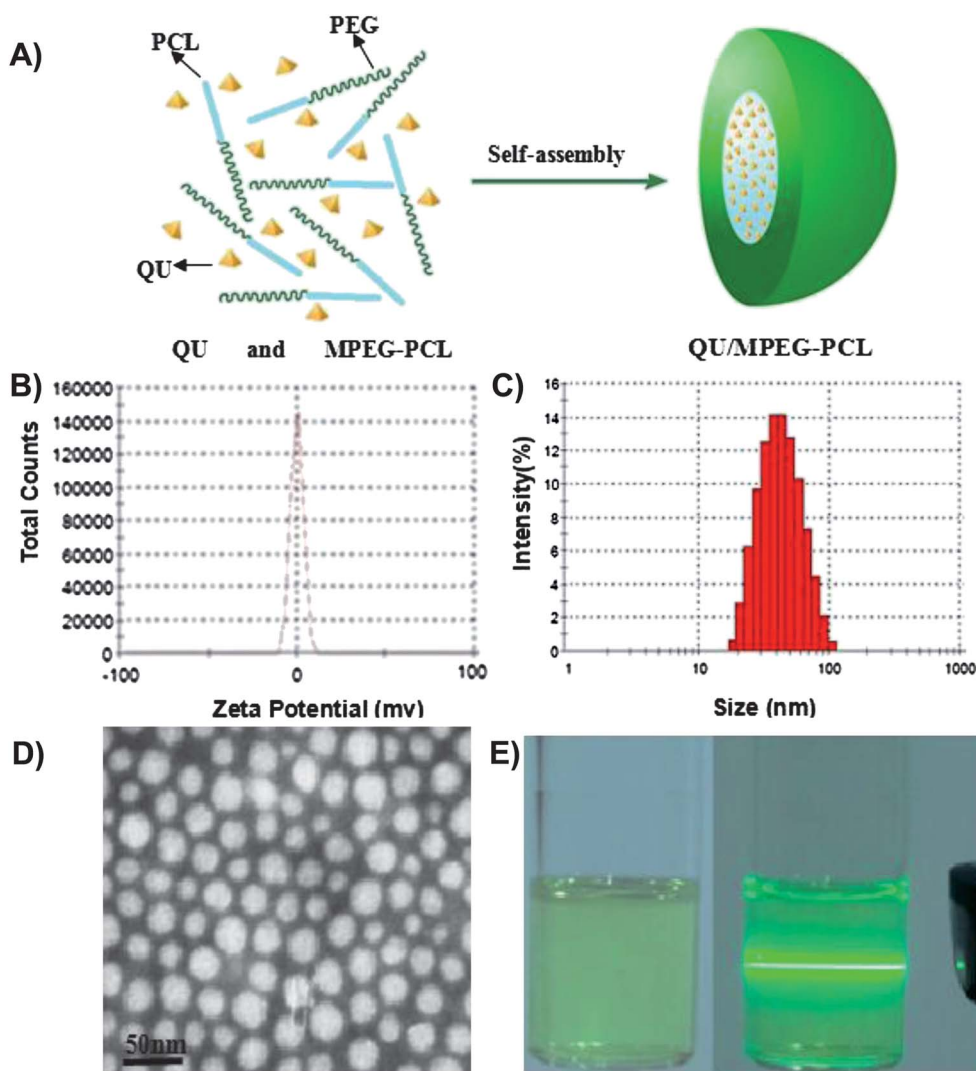


**Fig. 2** Preparation and characterization of the QU/MPEG-PCL micelles. (A) Preparation scheme of quercetin (QU) loaded in MPEG-PCL nanoparticles. MPEG-PCL and QU were co-dissolved in organic solvent, followed by evaporation to dryness under reduced pressure in a rotary evaporator, creating the QU and MPEG-PCL mixture. The QU and MPEG-PCL mixture was then hydrated in 0.9% normal saline, allowing QU and MPEG-PCL to self-assemble into QU/MPEG-PCL micelles. (B): The zeta potential spectrum of MPEG-PCL micelles; (C): the size distribution spectrum of QU/MPEG-PCL micelles; (D): a TEM image of QU/MPEG-PCL micelles; (E): photos of QU/MPEG-PCL in normal saline solution and the Tyndall effect of QU/MPEG-PCL micelles solution.

the particle size of micelles determined by DLS was always slightly larger than that determined by TEM.

One of the major purposes of the encapsulation of QU in MPEG-PCL micelles was to make QU completely dispersible in aqueous media. As can be seen from Fig. 2E, the solution of QU/MPEG-PCL micelles was uniform and had a clear Tyndall effect, indicating the existence of abundant nanoparticles that are completely dispersed in aqueous media.

### 3.2. Quercetin affected the cell viability

Human A2780S ovarian cancer cells were treated with various concentrations of quercetin from 0.12–30  $\mu\text{g mL}^{-1}$  for 24 and 48 h. Cell viability and cell proliferation were assessed by the MTT assay. As shown in Fig. 3A, quercetin caused a dose and time dependent reduction in cell viability. About 56.3% reduction in A2780S reduction in cell viability was seen at a dose of 30  $\mu\text{g mL}^{-1}$  after 48 h of incubation.

### 3.3. Quercetin inhibited cell colony formation

In order to further confirm the growth inhibitory effect of quercetin-treatment on ovarian cancer cells, A2780S cells were selected to detect growth curve status. These were plated (400) in 6-well plates and treated with quercetin (0, 7.5, 15, 30  $\mu\text{g mL}^{-1}$ ) for 24 h followed by 14 days of culture without treatment. Cell numbers were counted using a hemocytometer. As shown in Fig. 3B, the level of colony formation of A2780S cells was significantly inhibited by the increased concentrations of quercetin. The colony formation number showed a significant dose-dependent reduction by quercetin (Fig. 3C).

### 3.4. Antitumor activity of quercetin *in vivo*

To study the antitumor activity of quercetin *in vivo*, A2780S-bearing BALB/c nude mice were treated with quercetin at the

dose of 60  $\text{mg kg}^{-1}$ . Quercetin exhibited a significant antitumor activity in inhibiting tumor progress compared with the control.

Quercetin significantly decreased A2780S tumor volume by 66.14% *in vivo*, (Fig. 4A). Moreover, quercetin treatment was well tolerated without significant effects on body weight (Fig. 4B). Moreover, as presented in Fig. 4C, the weight of tumors in each treatment group also reflected that quercetin loaded MPEG-PCL micelles could effectively inhibit growth of the ovarian cancer compared with control. Furthermore, from photos of tumors in each treatment group (Fig. 4D), it was found that quercetin could inhibit the ovarian cancer growth.

### 3.5. Histological analysis by TUNEL assay and CD31

To study the mechanism associated with the anticancer activity of QU/MPEG-PCL nanoparticles *in vivo*, a TUNEL assay was carried out. As shown in Fig. 5A, many strongly positive nuclei identified as apoptotic could be observed in the quercetin treated tumor tissues, whereas such nuclei were rare in the control group, as observed by the TUNEL assay. Quercetin significantly decreased the fluorescence images of A2780S tumors by 27.7% compared with the control. This implied that apoptosis induction may be one mechanism of inhibiting ovarian cancer by the QU/MPEG-PCL *in vivo*.

Moreover, tumor sections of each treatment group were stained with CD31 for evaluating the microvessel density (MVD). The QU/MPEG-PCL treatment resulted in dramatic inhibition of angiogenesis in the tumors (Fig. 5B). We counted microvessel density in the xenograft tumors to determine whether *in vivo* administration of quercetin affects the microvessels. Microvessel density identified by immunoreactivity in the quercetin treatment group was 10 microvessel counts, which was significantly lower than that in the control group (40 microvessel counts). This implies that anti-angiogenesis may be another mechanism of inhibiting ovarian cancer by the quercetin *in vivo*.

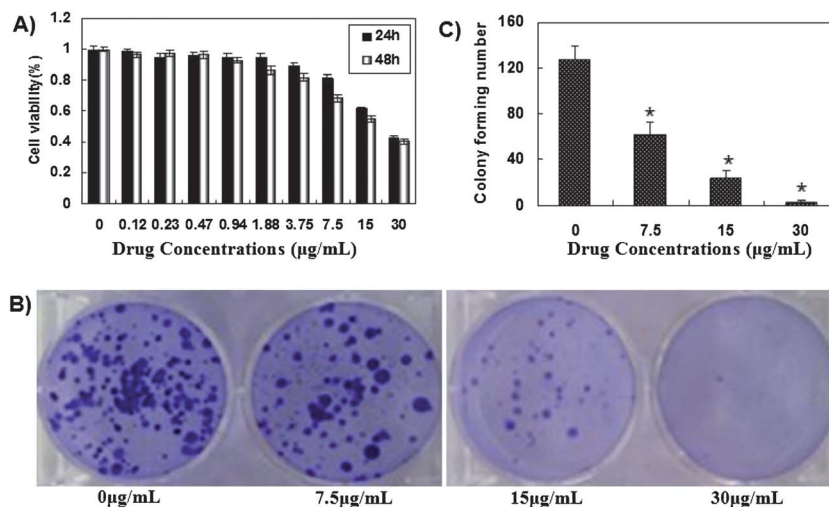


**Fig. 3** The anticancer activity of quercetin on A2780S ovarian cancer cells *in vitro*: (A) the inhibitory effect of quercetin on the proliferation of A2780S cancer cells. Cells were treated with increasing concentrations of quercetin (0.12–30  $\mu\text{g mL}^{-1}$ ) for 24 h and 48 h. Cell survival was measured by MTT. (B) Approximately 400 A2780S cells were plated in six-well plates and grown in complete DMEM medium. After 24 h, cells were washed once with serum-free DMEM medium and treated with different concentrations of quercetin in DMEM medium. After 24 h of treatment, cells were washed once with SFR medium and cultured in complete DMEM medium for various times. (C) Cells were harvested for colony formation counting using Gene Snap Automatic Colony Counter Software. An asterisk denotes significant differences between treatment groups ( $p < 0.05$ ).

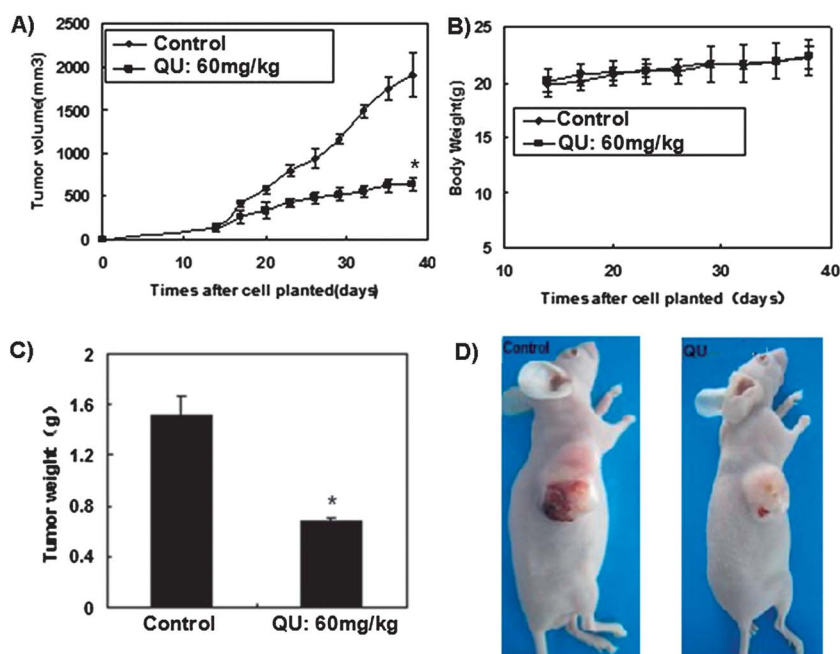


**Fig. 4** Quercetin inhibits ovarian cancer *in vivo*. Quercetin inhibits the growth of established A2780s tumor xenografts in athymic nude mice. Tumor volume and weights of A2780S (A and B) was measured on the indicated days. (C): The weight of tumor; (D): the representative photos of tumors in each treatment group. This indicated that quercetin can inhibit ovarian cancer growth *in vivo*. An asterisk denotes significant differences between treatment groups ( $p < 0.05$ ).

### 3.6. Apoptosis induced by quercetin

To determine whether quercetin reduced cell number by inducing apoptosis, the Hoechst 33342 assay was performed. Using Hoechst staining, an increased level of nuclear fragmentation and apoptotic bodies were detected in cells treated with quercetin (Fig. 6A). Morphological change of A2780S cells treated by quercetin was observed through Hoechst 33342 staining. The

features of apoptotic cells were a bright-blue fluorescent condensed nucleus, reduction of cell volume and nuclear fragmentation (Fig. 6A).

Moreover, the percentage of Annexin V positive cells in quercetin-treated group increased in a concentration-dependent manner. The apoptosis rate was 22.64% and 30.89%, respectively (shown in Fig. 6B), when cells were treated with 15  $\mu\text{g mL}^{-1}$  and 30  $\mu\text{g mL}^{-1}$  quercetin for 24 h.

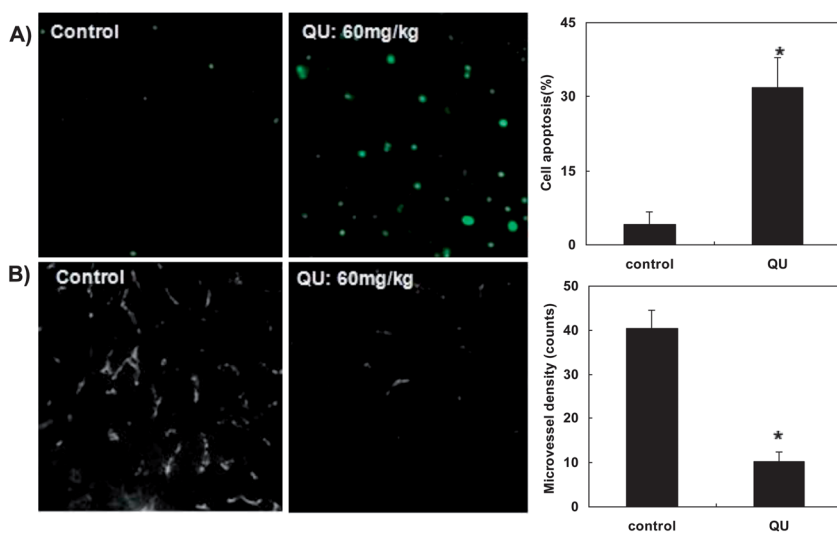


**Fig. 5** The TUNEL assay and the CD31 assay. Tumor sections of each treatment group were stained with TUNEL for the cell apoptosis assay and CD31 for evaluating the microvessel density (MVD). The quercetin treatment resulted in dramatic cell apoptosis and inhibition of angiogenesis in the tumors. This implies that inducing cancer cell apoptosis and anti angiogenesis may be mechanisms of inhibiting ovarian cancer by quercetin *in vivo*. An asterisk denotes significant differences between treatment groups ( $p < 0.05$ ).

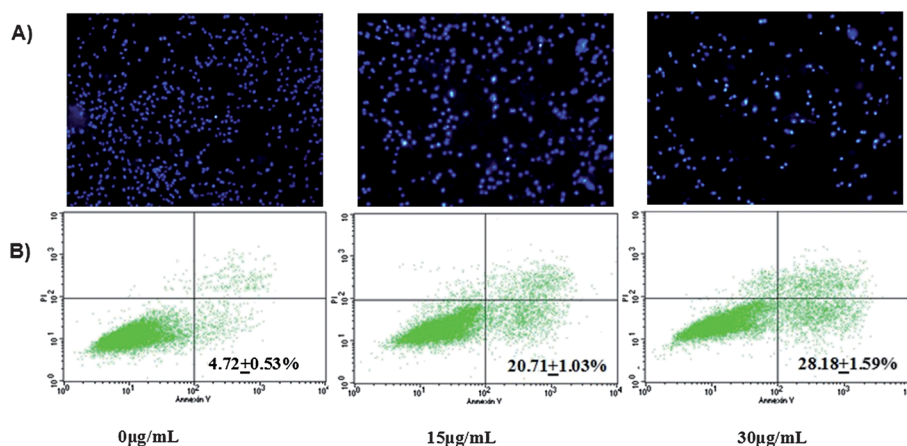


**Fig. 6** Detection of apoptosis in A2780 cells by Hoechst staining (A) and FCM (B). Cells were cultured on cover-slips and exposed to quercetin (0, 15 or 30  $\mu\text{g mL}^{-1}$ ) for 24 h. Cells were washed, fixed, stained with Hoechst 33258, and then observed under a fluorescent microscope.

### 3.7. Effects of quercetin on mitochondrial potential

A key step in the intrinsic apoptotic pathway is the damage of mitochondria to activate Apaf-1, which turns on the caspase cascade. An important event in the intrinsic apoptosis pathway is the mitochondrial membrane permeability disruption and loss of mitochondrial potential. As shown in Fig. 7, a decrease of Rh123 accumulation in A2780S cells was detected following quercetin treatment compared with the control ( $p < 0.05$ ), indicating the collapse of the mitochondrial membrane potential induced by quercetin.

### 3.8. Effect of quercetin on the mitochondrial apoptosis pathway

To further characterize quercetin-induced apoptosis and to investigate which apoptotic pathway quercetin activated, we examined caspase-3 and caspase-9, the apical proteases in the extrinsic pathways. As shown in Fig. 8A, procaspase-3 and procaspase-9 decreased significantly after quercetin exposure for 48 h in A2780S cells; moreover, the levels of cleaved caspase-3 and caspase-9 increased in a concentration-dependent manner. Collectively, we proposed that quercetin triggers apoptosis through the intrinsic pathway but not the extrinsic pathway.

### 3.9. Effect of quercetin on pro-apoptotic protein Bax expression

We examined pro-apoptotic protein Bax expression levels in A2780S cells after quercetin treatment for 48 h by Western

blotting analysis. As shown in Fig. 8B, Bax decrease was observed after quercetin treatment, which was also in agreement with the result of the change of mitochondrial potential.

### 3.10. Effect of quercetin on anti-apoptotic proteins MCL-1 and Bcl-2 expressions

We examined Bcl-2 and MCL-1 expression levels in A2780S cells after quercetin treatment for 48 h by Western blotting analysis. As shown in Fig. 8C, MCL-1 and Bcl-2 decrease were observed after quercetin treatment, which was in agreement with the results of the change of mitochondrial potential.

### 3.11. Effect of quercetin on MAPK and Akt activity

The p44/42 MAPK and Akt are known to play an important role in cell growth and apoptosis. We then measured the expression levels of Akt/p-Akt and MAPK/p-MAPK after quercetin exposure in A2780S cells. Interestingly, we found a remarkable decrease in the level of phosphorylated Akt and phosphorylated-MAPK (Fig. 8D). However, the levels of total Akt and MAPK were unaffected by quercetin.

## 4. Discussions

A large variety of polyphenolic compounds from vegetables and fruits have evoked considerable attention because of their multiple biological properties. Flavonoids have potent

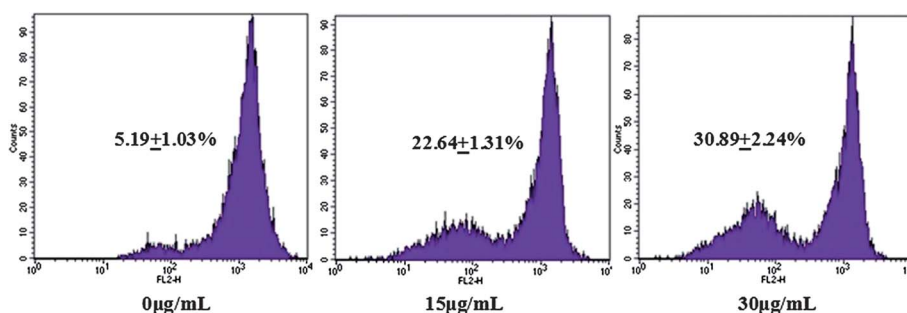


**Fig. 7** The mitochondrial transmembrane potential assay. A2780S cells were treated with quercetin for 24 h, and were stained by Rh123 to detect the change of mitochondrial transmembrane potential by flow cytometry. Data were the representative from three parallel experiments.

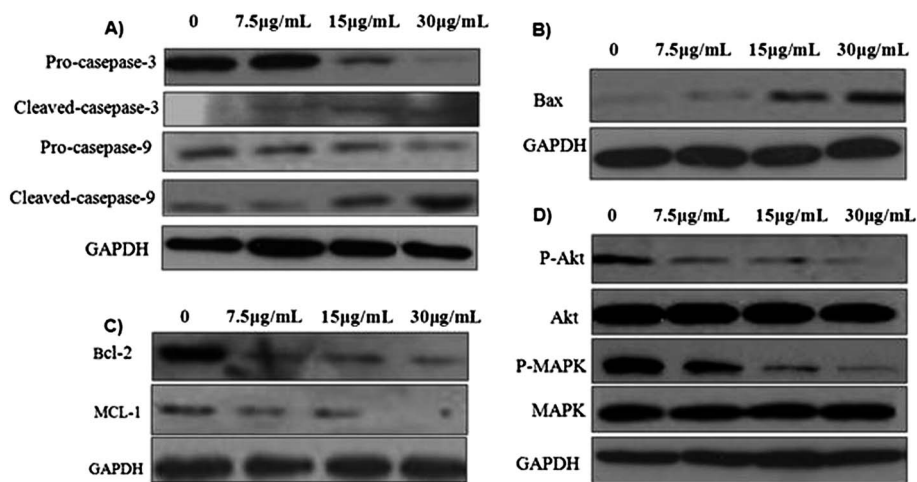


**Fig. 8** The effect of quercetin on apoptosis related proteins by Western blotting analysis. A2780S cells were exposed to quercetin for 48 h and cell extract proteins subjected to Western blotting analysis. (A) The effect of quercetin on caspase-3 and caspase-9. (B) The expression level of Bax in A2780S affected by quercetin was analyzed. (C) The expression levels of Bcl-2 and MCL-1 in A2780S affected by quercetin were analyzed. (D) The phosphorylation of Akt and p44/42 MAPK in A2780S were inhibited by quercetin. Data were the representative from three parallel experiments.

anti-proliferative, anti-neoplastic properties, and antioxidant activity, and it has been suggested that they prevent chronic diseases, such as cancer.<sup>33,34</sup> Ovarian cancer has a high incidence and high mortality; thus, it is necessary to develop new protocols for ovarian cancer therapy. Quercetin is a member of the flavonoids with potential application in cancer therapy.

However, quercetin is hydrophobic with poor water solubility, which limits its application in oral administration; but oral administrated quercetin always had a very low bioavailability. Despite the anticancer activity and mechanism of quercetin on ovarian cancer being revealed *in vitro*, potential clinical application of quercetin in ovarian cancer therapy was still restricted because of the poor water solubility of quercetin. Therefore, developing an aqueous formulation for quercetin is interesting. To address this challenge, liposomal quercetin and PLGA-quercetin have been described.<sup>34,35</sup> Liposomal quercetin is water soluble, but its diameter is relatively large. The liposomes with a large particle size are not easily absorbed, along with a relatively low bioavailability. Although the particle size of PLGA nano-quercetin is small, its encapsulation rate is relatively low. In this study, in order to solve the poor water-solubility of quercetin, MPEG-PCL micelles were used to deliver quercetin. In this protocol, quercetin was encapsulated into MPEG-PCL micelles by self-assembly methods (shown in Fig. 2A), rendering the complete dispersion of quercetin in water. Moreover, a mouse ovarian cancer subcutaneous model was employed to investigate the effect of quercetin on tumor growth inhibition. Results indicated that intravenous administration of MPEG-PCL micelle-encapsulated quercetin significantly suppressed the growth of A2780S ovarian cancer *in vivo* (shown in Fig. 4).

Moreover, to study the mechanism associated with the anti-cancer activity of quercetin *in vivo*, a TUNEL assay was carried out. As shown in Fig. 5A, many strongly positive nuclei identified as apoptotic could be observed in the quercetin-treated ovarian tumor tissues, whereas such nuclei were rare in control groups observed through the TUNEL assay. Also, tumor sections of

each treatment group were stained with CD31 for evaluating the microvessel density (MVD). The quercetin treatment resulted in dramatic inhibition of angiogenesis in the tumors (Fig. 5B). This implies that anti-angiogenesis may be another mechanism of inhibiting ovarian cancer by quercetin *in vivo*.

Quercetin showed anticancer activity against ovarian cancer, and previous studies have shown that quercetin can inhibit colony formation of cells from four primary ovarian tumors.<sup>36</sup> But the anticancer effect and molecular mechanism of quercetin on ovarian cancer have not been well known. In this study, we hypothesized that quercetin should have some anti-cancer effects on ovarian cancer, associated with regulating the expression of various proteins to controlling tumor suppression and oncogenesis. Firstly, MTT and colony formation experiments were employed to verify the influence of quercetin on ovarian cancer. We found that quercetin could inhibit the growth of ovarian cancer *in vitro*. Moreover, we have detected that quercetin can induce apoptosis in ovarian cancer by FCM. Apoptosis, which is also known as programmed cell death, plays a crucial role in the maintenance of cell homeostasis. Apoptosis may occur *via* a death receptor-dependent (extrinsic) or independent (intrinsic or mitochondrial) pathway. In order to determine the mechanism of quercetin induced apoptosis in ovarian cancer, we examined changes of mitochondrial potential and a series of protein changes, such as caspase-3, caspase-9, MCL-1, Bax and so on. Mitochondrial potential change is one of the characteristics of the mitochondrial pathway (shown in Fig. 9) of apoptosis.<sup>37</sup> Mitochondrial potential was decreased, as observed by FCM with Rh123 staining. Further, caspase-3 and caspase-9 are the downstream molecules in the mitochondrial pathway of apoptosis.<sup>38</sup> We found that procaspase-3 and procaspase-9 decreased significantly and the levels of cleaved caspase-3 and cleaved caspase-9 increased after quercetin exposure for 48 h in A2780S cells. This indicated that the apoptosis mechanism may be by the mitochondrial pathway. The mechanism of quercetin-induced apoptosis in ovarian cancer is consistent with breast cancer and liver cancer.

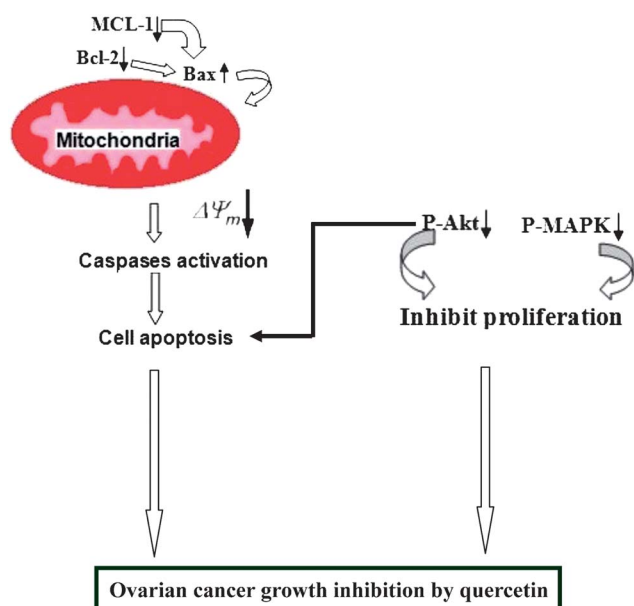


**Fig. 9** The mechanism of quercetin for inhibiting ovarian cancer growth. Quercetin inhibited ovarian cancer A2780S cell growth, which was associated with an apoptosis-inducing effect and proliferation inhibitory effect. Firstly, the apoptosis-inducing effect of quercetin was associated with its apoptosis-inducing effect by activating caspase-3 and caspase-9. Exposure of A2780S to quercetin also resulted in anti-apoptotic proteins MCL-1 and Bcl-2 downregulation, pro-apoptotic protein Bax upregulation, and mitochondrial transmembrane potential change in the mitochondrial apoptotic pathway. Moreover, the decrease of phosphorylated p44/42 mitogen-activated protein kinase (P-MAPK) and phosphorylated Akt was associated with the mechanism of the proliferation inhibitory effect shown by quercetin.

The regulation of mitochondrial apoptosis pathway is complex and multifaceted. The Bcl-2 family, including the anti-apoptotic Bcl-2 and MCL-1 and the pro-apoptotic Bax, are the central regulators of this process.<sup>39,40</sup> The levels of anti-apoptotic proteins Bcl-2 and MCL-1 are decreased and pro-apoptotic protein Bax is normally increased, which are the markers of the cancer cell apoptosis. It translocates to the outer mitochondrial membrane after suffering apoptotic stimuli, inducing mitochondrial membrane permeabilization. In the present study, we found that MCL-1 and Bcl-2 was down-regulated while Bax was up-regulated in A2780S cells treated with quercetin. We assume that MCL-1, Bcl-2 and Bax are involved in the mitochondrial potential change after quercetin treatment. This indicated that the apoptosis mechanism of ovarian cancer cell by quercetin was *via* the mitochondrial pathway.

Akt is involved in the regulation of diverse cellular processes, including glucose metabolism, cell growth, cell proliferation, angiogenesis, and apoptosis.<sup>41–43</sup> Its phosphorylation has been considered a critical factor in the aggressiveness of cancer.<sup>44</sup> Phosphorylated Akt can inhibit cell apoptosis and promote cell proliferation. Quercetin induced inactivation of Akt by decreasing the level of phosphorylated Akt in a concentration-dependent manner, contributing to the promotion of apoptosis and inhibition of cell proliferation.

In this study, we found that quercetin remarkably decreased the phosphorylated levels of both Akt and p44/42 MAPK,

indicating the involvement of Akt and MAPK in quercetin antitumor activity. Therefore, our findings are consistent with these previous studies. It is well known that p44/42 MAPK promote cell proliferation and mediate cell survival by the RAS-RAF-MEK-MAPK pathway. Though it is not involved in quercetin-induced apoptosis, it may reduce A2780S viability *via* inhibiting proliferation.

## 5. Conclusions

Quercetin exhibited anticancer activity in A2780S ovarian cancer cells. Encapsulation of quercetin in MPEG-PCL micelles rendered quercetin completely dispersible in water. Intravenous administration of MPEG-PCL micelle encapsulated quercetin significantly suppressed the growth of established xenograft A2780S ovarian tumors through causing cancer cell apoptosis and inhibiting angiogenesis *in vivo*. Activating caspase-3 and caspase-9 contributed to induction of apoptosis in A2780S cells by quercetin. Moreover, quercetin-induced apoptosis of A2780S cells through the mitochondrial apoptotic pathway was revealed. Otherwise, quercetin treatment decreased phosphorylated p44/42 mitogen-activated protein kinase and phosphorylated Akt, contributing to inhibit A2780S cell proliferation. This work may provide a proof-of-principle for treating ovarian cancer with QU/MPEG-PCL micelles.

## Acknowledgements

This work was supported by the Specialized Research Fund for the Doctoral Program of Higher Education (20110181120087), the National Key Basic Research Program (973 Program) of China (2011CB910703), the Fund from Science and Technology Department of Sichuan Province (2010SZ0156).

## References

- 1 American Cancer Society, *Cancer Facts & Figures 2011*, American Cancer Society, Atlanta, 2011.
- 2 A. Jemal, F. Bray, M. M. Center, J. Ferlay, E. Ward and D. Forman, Global cancer statistics, *Ca-Cancer J. Clin.*, 2011, **61**(2), 69–90.
- 3 R. Siegel, M. A. Deppa Naishadham and D. V. M. Ahmedin Jemal, *Cancer Statistics, 2012*, CA, 2012, pp. 10–29.
- 4 B. T. Hennessy, R. L. Coleman and M. Markman, Ovarian cancer, *Lancet*, 2009, **374**(9698), 1371–1382.
- 5 L. Gilbert, O. Basso and J. Sampalis, *et al.* Assessment of symptomatic women for early diagnosis of ovarian cancer: results from the prospective DOvE pilot project, *Lancet Oncol.*, 2012, **3**(13), 285–291.
- 6 M. Vanneman and G. Dranoff, Combining immunotherapy and targeted therapies in cancer treatment, *Nat. Rev. Cancer*, 2012, **12**, 237–251.
- 7 R. Dantzer, M. W. Meagher and C. S. Cleeland, Translational approaches to treatment-induced symptoms in cancer patients, *Nat. Rev. Clin. Oncol.*, 2012, **9**, 414–426.
- 8 C. J. Lord and A. Ashworth, The DNA damage response and cancer therapy, *Nature*, 2012, **481**, 287–294.
- 9 A. Ślusarz, N. S. Shenouda and M. S. Sakla, *et al.* Common botanical compounds inhibit the Hedgehog signaling pathway in prostate cancer, *Cancer Res.*, 2010, **70**, 3382–3391.
- 10 S. Cheng, N. Gao and Z. Zhang, *et al.* Quercetin induces tumor-selective apoptosis through downregulation of Mcl-1 and activation of Bax, *Clin. Cancer Res.*, 2010, **16**, 5679–5692.
- 11 F. Sahoulia, K. Drosopoulos and L. Doubravska, *et al.* Quercetin enhances TRAIL-mediated apoptosis in colon cancer cells by inducing the accumulation of death receptors in lipid rafts, *Mol. Cancer Ther.*, 2007, **6**, 2591–2599.

- 12 M. Comalada, D. Camuesco and S. Sierra, *et al.* *In vivo* quercitrin anti-inflammatory effect involves release of quercetin, which inhibits inflammation through down-regulation of the NF- $\kappa$ B pathway, *Eur. J. Immunol.*, 2005, **35**, 584–592.
- 13 D. J. L. Jones, J. H. Lamb and R. D. Verschoyle, *et al.* Characterisation of metabolites of the putative cancer chemopreventive agent quercetin and their effect on cyclooxygenase activity, *Br. J. Cancer*, 2004, **91**, 1213–1219.
- 14 P.-C. Kuo, H.-F. Liu and J.-I. Chao, Survivin and p53 Modulate quercetin-induced cell growth inhibition and apoptosis in human lung Carcinoma cells, *J. Biol. Chem.*, 2004, **279**, 55875–55885.
- 15 B. Plaumann, M. Fritsche, H. Rimpler, G. Brandner and R. D. Hess, Flavonoids activate wild-type p53, *Oncogene*, 1996, **13**, 1605–1614.
- 16 G. Ferrandina, G. Almadori, N. Maggiano, P. Lanza, C. Ferlini, P. Cattani, M. Piantelli, G. Scambia and F. O. Ranelletti, Growth-inhibitory effect of tamoxifen and quercetin and presence of type II estrogen binding sites in human laryngeal cancer cell lines and primary laryngeal tumors, *Int. J. Cancer*, 1998, **77**, 747–754.
- 17 M. Yoshida, M. Yamamoto and T. Nikaido, Quercetin arrests human leukemic T-cells in late G1 phase of the cell cycle, *Cancer Res.*, 1992, **52**, 6676–6681.
- 18 R. G. Beniston and M. S. Campo, Quercetin elevates p27Kip1 and arrests both primary and HPV16 E6/E7 transformed human keratinocytes in G1, *Oncogene*, 2003, **22**, 5504–5514.
- 19 S. Tottey, K. J. Waldron and S. J. Firbank, Protein-folding location can regulate manganese-binding versus copper- or zinc-binding, *Nature*, 2008, **455**, 1138–1142.
- 20 C. Voelkel-Johnson, TRAIL-mediated signaling in prostate, bladder and renal cancer, *Nat. Rev. Urol.*, 2011, **8**, 417–427.
- 21 D. T. Coleman, R. Bigelow and J. A. Cardelli, Inhibition of fatty acid synthase by luteolin post-transcriptionally down-regulates c-Met expression independent of proteosomal/lysosomal degradation, *Mol. Cancer Ther.*, 2009, **8**, 214–224.
- 22 X. Li, Z. Zhang and J. Li, *et al.* Diclofenac/biodegradable polymer micelles for ocular applications, *Nanoscale*, 2012, **4**, 4667–4673.
- 23 M. C. Parrott and J. M. DeSimone, Drug delivery: relieving PEGylation, *Nat. Chem.*, 2012, **4**, 13–14.
- 24 G. Guo, S. Z. Fu and L. X. Zhou, *et al.* Preparation of curcumin loaded poly( $\epsilon$ -caprolactone)-poly(ethylene glycol)-poly( $\epsilon$ -caprolactone) nanofibers and their *in vitro* antitumor activity against Glioma 9L cells, *Nanoscale*, 2011, **3**, 3825–3832.
- 25 M. L. Gou, K. Men and J. A. Zhang, *et al.* Efficient inhibition of C-26 colon Carcinoma by VSVMP Gene delivered by biodegradable cationic nanogel derived from polyethyleneimine, *ACS Nano*, 2010, **4**(103–5584), 557.
- 26 J.-H. Park, L. Gu and G. V. Maltzahn, *et al.* Biodegradable luminescent porous silicon nanoparticles for *in vivo* applications, *Nat. Mater.*, 2009, **8**, 331–336.
- 27 M. L. Gou, K. Men and H. S. Shi, *et al.* Curcumin loaded biodegradable polymeric micelle for colon cancer therapy *in vitro* and *in vivo*, *Nanoscale*, 2011, **3**, 1558–1567.
- 28 M. Gou, X. Wei and K. Men, *et al.* PCL/PEG copolymeric nanoparticles: potential nanoplatforms for anticancer agent delivery, *Curr. Drug Targets*, 2011, **12**, 1131–1150.
- 29 B. L. Wang, X. Gao and K. Men, Treating acute cystitis with biodegradable micelle-encapsulated quercetin, *Int. J. Nanomed.*, 2012, **7**, 2239–2247.
- 30 W. Zhang, D. Trachootham and J. Liu, *et al.* Stromal control of cystine metabolism promotes cancer cell survival in chronic lymphocytic leukaemia, *Nat. Cell Biol.*, 2012, **14**, 276–286.
- 31 H. Jiang, N. Song and H. Xu, *et al.* Up-regulation of divalent metal transporter 1 in 6-hydroxydopamine intoxication is IRE/IRP dependent, *Cell Res.*, 2010, **20**, 345–356.
- 32 N. J. Allen, M. L. Bennett and L. C. Foo, *et al.* Astrocyte glypicans 4 and 6 promote formation of excitatory synapses via GluA1 AMPA receptors, *Nature*, **486**, 410–414.
- 33 Y.-Q. Wei, X. Zhao and Y. Kariya, *et al.* Induction of apoptosis by quercetin: involvement of heat shock protein, *Cancer Res.*, 1994, **54**, 4952–4957.
- 34 Z.-P. Yuan, L.-J. Chen and L.-Y. Fan, *et al.* Liposomal quercetin efficiently suppresses growth of solid tumors in murine models, *Clin. Cancer Res.*, 2006, **12**, 3193–3199.
- 35 S. Chakraborty, S. Stalin and N. Das, *et al.*, The use of nano-quercetin to arrest mitochondrial damage and MMP-9 upregulation during prevention of gastric inflammation induced by ethanol in rat, *Biomaterials*, 2012, **33**, 2991–3001.
- 36 G. Scambia, F. Ranelletti and P. Panici, Quercetin and hyperthermia produce a synergistic inhibitory effect on primary human ovarian-cancer cells, *Int. J. Oncol.*, 1992, **1**(3), 299–302.
- 37 J. E. Chipuk, G. P. McStay and A. Bharti, *et al.*, Sphingolipid metabolism cooperates with BAK and BAX to promote the mitochondrial pathway of apoptosis, *Cell*, 2012, **148**, 988–1000.
- 38 Z. Li, J. Jo and J.-M. Jia, *et al.*, Caspase-3 activation via mitochondria is required for long-term depression and AMPA receptor internalization, *Cell*, 2010, **5**, 859–871.
- 39 J.-C. Martinou and R. J. Youle, Mitochondria in apoptosis: bcl-2 family members and mitochondrial dynamics, *Dev. Cell*, 2011, **1**, 92–101.
- 40 F. Edlich, S. Banerjee, M. Suzuki and M. M. Cleland, *et al.*, Bcl-xL retrotranslocates Bax from the mitochondria into the cytosol, *Cell*, 2011, **145**, 104–116.
- 41 I. E. Wertz, Saritha Kusam and Cynthia Lam, *et al.*, Sensitivity to antitubulin chemotherapeutics is regulated by MCL1 and FBW7, *Nature*, 2011, **471**, 110–114.
- 42 M. Hanada, J. Feng and B. A. Hemmings, Structure, regulation and function of PKB/AKT-a major therapeutic target, *Biochim. Biophys. Acta, Proteins Proteomics*, 2004, **1697**, 3–16.
- 43 B. T. Hennessy, D. L. Smith, P. T. Ram, Y. Lu and G. B. Mills, Exploiting the PI3K/AKT pathway for cancer drug discovery, *Nat. Rev. Drug Discovery*, 2005, **4**, 988–1004.
- 44 V. Nogueira, Y. Park and C.-C. Chen, *et al.*, Akt determines replicative senescence and oxidative or oncogenic premature senescence and sensitizes cells to oxidative apoptosis, *Cancer Cell*, 2008, **14**, 458–470.